Variants of Seeded Region Growing*

Minjie Fan and Thomas C. M. Lee†

Department of Statistics, University of California, Davis, One Shields Avenue, Davis, CA 95616, U.S.A.

Abstract

Seeded region growing (SRG) is a fast, effective and robust method for image segmentation. It begins with placing a set of seeds in the image to be segmented, where each seed could be a single pixel or a set of connected pixels. Then SRG grows these seeds into regions by successively adding neighboring pixels to them. It finishes when all pixels in the image are assigned to one (and only one) region. The growing strategy of SRG implicitly assumes that pixels from the same region share the same greyvalue. As a first contribution, this paper develops new modifications to SRG so that this constant greyvalue assumption is relaxed. Since the growing strategy of SRG does not impose any constraints or restrictions on the shapes of the growing regions, quite often SRG would produce very rough segmentation boundaries even the true boundaries were smooth. The second contribution of this paper is the proposal of a stabilized SRG that encourages smoother boundaries and prevents the so-called leakage problem. All these new variants are conceptually simple and easy to implement. They are tested with simulated and real images, and are shown to have better performances than the original SRG.

Keywords: Image segmentation, Leakage prevention, Planar and quadratic surface modeling, Smooth boundary, Stabilized seeded region growing.

†Corresponding author: tcmlee@ucdavis.edu

1 Introduction

Image segmentation aims to locate the boundaries of objects contained in images. The seeded region growing (SRG) method proposed by [1] is a conceptually simple and yet an effective and robust technique for performing segmentation. Since its inception, it has been widely applied by researchers and practitioners to produce successful segmentation results for different real life problems; e.g., see [2–4] and [5]. In addition, various extensions and modifications have been proposed to improve the performance of SRG; e.g., see [6], [7, 8] and [9].

The main goal of this paper is to introduce three new variants of SRG to further improve its performance under the following two scenarios. Notice that an implicit assumption behind SRG is that all pixels within the same region share the same greyvalue. In other words, all regions in the image are of constant greyvalues, and can be modeled as horizontal planes. The first scenario this paper considers is when this constant greyvalue assumption is violated. To be more specific, the first contribution of this paper is the development of two SRG variants for which the regions are modeled as linear planes and quadratic surfaces, respectively. To the best of the authors' knowledge, there is no existing SRG based method that is designed to cope with linear and quadratic regions.

The second scenario happens when the signal–to–noise ratio of the image is low, or when the boundary between a region and its background is blurry. In this case the so-called leakage problem could occur, which would in turn produce poor segmentation results. As a second contribution, this paper proposes a SRG variant to circumvent this issue by encouraging smoother segmented region boundaries. It is noted that various SRG modifications have been proposed to produce smoother boundaries [e.g., 7, 8, 10], but a distinct advantage of the current proposal is that it can be easily paired with other variants developed in this paper.

The rest of this paper is organized as follows. In Section 2 the original SRG of [1] will first be reviewed, and then it will be modified for enhanced performances. All the new SRG variants will be empirically accessed through a sequence of images in Section 3. In general these new variants improve the results from the original SRG. Concluding remarks are given in Section 4.

2 Variants of Seeded Region Growing

2.1 The Original Seeded Region Growing

The original SRG [1] begins segmenting an image from a set of seeds. Each of these seeds could be a single pixel or a group of pixels, and they can be specified manually by a human operator or automatically by pre-processing steps [e.g., 3, 5]. These seeds are then allowed to grow and form regions in a manner to be described below. Finally the whole procedure finishes when the image is fully partitioned by all the growing regions. Object boundaries are obtained as the boundaries of the final regions.

A more precise description of the original SRG is as follows. Suppose initially there are N seeds, and they are collected in N sets, $A_1, A_2, \cdots, A_N$. Let T be the set of all pixels which are adjacent to at least one of the pixels in A_i's:

$$T = \left\{ x \notin \bigcup_{i=1}^{N} A_i | \text{nbr}(x) \cap \bigcup_{i=1}^{N} A_i \neq \emptyset \right\},$$

where $\text{nbr}(x)$ is the set of all immediate neighbors of pixel x. At each time step, the growing process selects one pixel x from T and adds it to one of its neighboring regions; A_i is a neighboring region of x if $\text{nbr}(x) \cap A_i \neq \emptyset$. This pixel is chosen according to some homogeneity criterion. In [1] the criterion is to choose the pixel whose greyvalue is closest to the average greyvalue of one of its neighboring growing regions, say A_p where $1 \leq p \leq N$. This pixel will then be added to that region, and both T and A_p will be updated. This process continues until all the pixels in the image are allocated to one and only one of the growing regions. The criterion of [1] ensures that the grey values for each final region are as homogeneous as possible under the connectivity constraint.

The following notation will prove to be useful in subsequent sections. Denote the pixels of the growing region R under consideration as $R = \{r_1, r_2, \cdots, r_n\}$; i.e., there are n pixels. Let $g(x)$ be the greyvalue of pixel x. With this notation, the original SRG is to choose the pair of (x, R) such that the following criterion is minimized:

$$\delta_{\text{O}}(x, R) = \left| g(x) - \frac{1}{n} \sum_{i=1}^{n} g(r_i) \right| = |g(x) - \bar{r}|,$$

where $\bar{r} = \frac{1}{n} \sum_{i=1}^{n} g(r_i)$ is the averaged greyvalue of R. In below modifications to $\delta_{\text{O}}(x, R)$ are presented

to improve the performance of the original SRG.

2.2 Linear Seeded Region Growing

As hinted before, the use of $\delta_{\mathrm{O}}(x, R)$ implicitly assumes that the greyvalues of any region in the image can be well approximated by a single constant value. This subsection relaxes this assumption by modeling the greyvalues with a linear plane (i.e., a plane with a non-zero slope).

Let the numbers of rows and columns of an image be n_r and n_c respectively. Then the coordinate of a pixel located at the i-th row and j-th column is $(i/n_r, j/n_c)$. The greyvalue of a pixel is modeled as $a_1(i/n_r) + a_2(j/n_c) + a_3 + \epsilon$, where a_1, a_2 and a_3 are coefficients of the corresponding plane, and ϵ is a zero-mean error term, usually assumed to be identically and independently distributed. It is assumed that pixels of the same region share the same a_1, a_2 and a_3.

To generalize $\delta_{\mathrm{O}}(x, R)$, first obtain least squares estimates of the coefficients using the pixels in R; denote the resulting estimates as $\hat{a}_1$, $\hat{a}_2$ and $\hat{a}_3$. If the coordinate of pixel x is $(i_x/n_r, j_x/n_c)$, then the new homogeneity criterion is

$$\delta_{\mathrm{L}}(x, R) = \left| g(x) - \left\{ \hat{a}_1 \left(\frac{i_x}{n_r} \right) + \hat{a}_2 \left(\frac{j_x}{n_c} \right) + \hat{a}_3 \right\} \right|.$$

Thus at each time step the pair of (x, R) that minimizes $\delta_{\mathrm{L}}(x, R)$ is first sought, and the region R is grown by adding x into it. Note that the estimates $(\hat{a}_1, \hat{a}_2, \hat{a}_3)$ will need to be re-calculated whenever a new x is added to R. However, fast updating formulae exist so computationally it is fast. In sequel this new variant is termed linear seeded region growing (Linear-SRG).

2.3 Quadratic Seeded Region Growing

Quadratic seeded region growing (Quadratic-SRG) is similar to Linear-SRG. The only difference is that the regions are modeled by quadratic surfaces instead of linear planes. Specifically, the greyvalues of a region are assumed to follow $b_1(i/n_r)^2 + b_2(i/n_r)(j/n_c) + b_3(j/n_c)^2 + b_4(i/n_r) + b_5(j/n_c) + b_6 + \epsilon$ with $b_1, \cdots, b_6$ being the coefficients of the surface. For any pair (x, R), denote the least squares estimates of these coefficients as $\hat{b}_1, \cdots, \hat{b}_6$. The corresponding homogeneity criterion is:

$$\delta_{\mathrm{Q}}(x, R) = \left| g(x) - \left\{ \hat{b}_1 \left(\frac{i_x}{n_r} \right)^2 + \hat{b}_2 \left(\frac{i_x j_x}{n_r n_c} \right) + \hat{b}_3 \left(\frac{j_x}{n_c} \right)^2 + \hat{b}_4 \left(\frac{i_x}{n_r} \right) + \hat{b}_5 \left(\frac{j_x}{n_c} \right) + \hat{b}_6 \right\} \right|. \quad (1)$$

It is straightforward to see that both Linear-SRG and Quadratic-SRG generalize the original SRG, as both $\delta_{\mathrm{L}}(x, R)$ and $\delta_{\mathrm{Q}}(x, R)$ reduce to $\delta_{\mathrm{O}}(x, R)$ when the appropriate coefficients are set to zero. In other words, both Linear-SRG and Quadratic-SRG can handle regions of constant greyvalues, as the least squares estimates of the corresponding coefficients will be close to zero.

2.4 Stabilized Seeded Region Growing

When growing a region, the original SRG does not impose any constraint or restriction on the shape or boundary of the region. When the signal-to-noise ratio is low, the final segmented boundaries could be very rough even though if the true boundaries were smooth. In addition, the so-called leakage problem could occur. This leakage problem refers to the situation when the greyvalues of two adjacent objects are similar, and the growing region of one object breaks the true boundary and enters into the other object through a narrow spike. This subsection proposes a new SRG variant that encourages smoother boundaries and also aims to prevent the leakage problem. When comparing to previous attempts [e.g., 7, 10], one advantage of the current proposal is that it can be straightforwardly paired with any of the SRG variants described above. The new variant is termed stabilized seeded region growing (Stabilized-SRG).

During the growth process, when determining which pixel x should be added to one of the growing regions, Stabilized-SRG does not only consider the greyvalue of x, but it also takes the greyvalues of a set of neighboring pixels of x into account. By simultaneously considering the greyvalues of these neighboring pixels, as to be shown below, will have a stabilizing effect on how the regions should be grown. This set of neighboring pixels are defined as all pixels covered by the square of size $(2L + 1) \times (2L + 1)$ centered at x; the choice of L will be discussed below. In below this set of neighboring pixels are denoted as $Y_L = \{y_{jk} | -L \leq j, k \leq L\}$. Note that $y_{00} = x$, but for convenience, y_{00} is used in Y_L instead of x. See Figure 1 for an example with $L = 1$. With this setup, at each step Stabilized-SRG adds x to R if the following criterion is minimized:

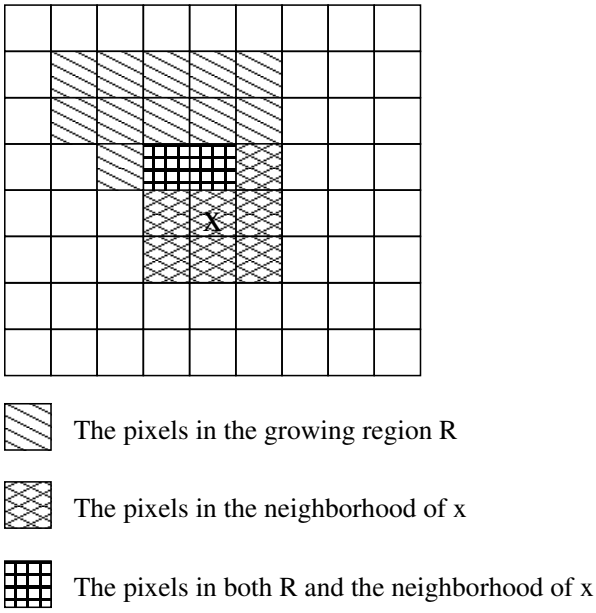

Figure 1: An illustration of the set of neighboring pixels Y_L (including x itself).

$$\begin{aligned}\delta_{\mathrm{S}}(x,R,Y_L) &= \frac{1}{(2L+1)^2}\left\{\sum_{j,k=-L,\cdots,L;j^2+k^2\neq 0}\left|g(y_{jk})-\frac{1}{n}\sum_{i=1}^{n}g(r_i)\right|+\left|g(x)-\frac{1}{n}\sum_{i=1}^{n}g(r_i)\right|\right\}\\ &= \frac{1}{(2L+1)^2}\left\{\sum_{j,k=-L}^{L}\left|g(y_{jk})-\frac{1}{n}\sum_{i=1}^{n}g(r_i)\right|\right\}\\ &= \frac{1}{(2L+1)^2}\left\{\sum_{j,k=-L}^{L}|g(y_{jk})-\bar{r}|\right\},\end{aligned} \tag{2}$$

where $\bar{r} = \frac{1}{n}\sum_{i=1}^{n} g(r_i)$ is the averaged greyvalue of R. From the definition of $\delta_{\mathrm{S}}(x,R,Y_L)$, the stabilizing effect on the growth is apparent: it favors adding pixel x to a growing region if the greyvalue of x is similar to its surrounding pixels. This property tends to produce smoother boundaries.

Notice that when $L = 0$, $\delta_{\mathrm{S}}(x,R,Y_L)$ reduces to $\delta_{\mathrm{O}}(x,R)$, and therefore the original SRG is a special case of Stabilized-SRG. Also notice that Stabilized-SRG can be paired with Linear-SRG or Quadratic-SRG by modifying $\delta_{\mathrm{S}}(x,R,Y_L)$, in a similar fashion as $\delta_{\mathrm{O}}(x,R)$ was modified to $\delta_{\mathrm{L}}(x,R)$ and $\delta_{\mathrm{Q}}(x,R)$. The parameter L, which determines the size of the neighborhood, also determines the extent to which the boundary will be smoothed. The larger the value of L, the smoother the boundary. The optimal choice of L will, amongst other factors, depend on the objects to be segmented. In practice it can be chosen by an operator in an interactive manner, or pre-specified if prior knowledge about the image is available.

2.5 Practical Implementation

One attractive feature shared by all of the above SRG variants is that they are conceptually simple and their practical implementation does not involve any computationally expensive operations (e.g., function optimization using iterative methods). In fact their practical implementation is similar to that of the original proposal of [1], which consists of the following steps:

Step 0: Construct the initial growing region sets $A_1, A_2, \cdots, A_N$, each of which is composed of the pre-specified seeds. Label each seed pixel by the index of its corresponding set.

Step 1: For each set A_i, compute the value of the homogeneity criterion δ for all its immediate, unlabeled neighbors. The criterion δ can be any of δ_{O}, δ_{L}, δ_{Q} or δ_{S}.

Step 2: Take the pixel with the smallest value of δ from these immediate neighbors and add it to its corresponding growing region set. Label this pixel with the index of its corresponding set. If all the pixels in the image are labelled, the algorithm finishes. Otherwise, update all A_i's and go to Step 1.

Lastly it is worth mentioning that, depending on the nature of the image to be segmented, in practice one could achieve better results by mixing the above growing strategies; e.g., grow some regions with Linear-SRG, while others with Stabilized-SRG. Section 3.3 below presents some empirical results for this mixing strategy.

2.6 Segmentation Evaluation Approach

Typically, there are two types of evaluation methods to assess whether an algorithm produces reasonable segmentation results or whether it segments images more accurately than other methods. They are supervised evaluation and unsupervised evaluation. Supervised evaluation is subjective in the sense that the quality of segmentation is evaluated by a human visually. In contrast, unsupervised evaluation is more objective and thus more preferable under certain circumstances when the quality of segmentation is difficult to judge merely by eyeballs. Readers who are interested in image segmentation evaluation are referred to [11].

For Stabilized-SRG, the evaluation of the quality of segmentation is based on whether leakage happens and whether boundaries are smooth, which can be examined straightforwardly by supervised

evaluation. But for the other two variants: Linear-SRG and Quadratic-SRG, we propose an unsupervised evaluation method based on F *evaluation function* ([12]). Suppose a digital image I has been segmented into N regions, denoted as $A_j, j = 1, 2, \cdots, N$. For region j, denote its area (measured by the number of pixels) as $S_j = |A_j|$. Suppose the true geometric shape of each region is either a linear plane or a quadratic surface. By fitting the corresponding parametric form to the greyvalues of the pixels in region j, we obtain the fitted greyalues $\hat{g}(x)$, where $x \in A_j$. The generalized F *evaluation function* is defined as

$$F_g(I) = \sqrt{N} \sum_{j=1}^{N} \frac{e_j^2}{\sqrt{S_j}},$$

where $e_j^2 = \sum_{x \in A_j} (g(x) - \hat{g}(x))^2$. Smaller F_g indicates better segmentation results.

3 Empirical Results

In this section the proposed SRG variants are applied to different simulated and real images to illustrate their empirical performances.

3.1 Simulated Images

Three artificial images, all of size 100×100, are used. The greyvalue $I_1(i, j)$ of the first image at the i-th row and j-th column is given by

$$I_1(i,j) = \begin{cases} 2(i-50) + 10 + \epsilon, & i \in [1, 50] \\ 10 + \epsilon, & i \in [51, 100] \end{cases},$$

where the error term ϵ is normally distributed with mean 0 and standard deviation $\sigma = 2$. This is a noisy image consisting of two neighboring planar surfaces with boundary at $i = 50$. The first plane is with a non-zero slope while the second plane is horizontal. Both the original SRG and the proposed Linear-SRG were applied to segment this image. The results are given in Figure 2. One can see that Linear-SRG outperformed the original SRG as its segmented boundary is much closer to $i = 50$.

The second artificial image $I_2(i, j)$ is composed of two quadratic surfaces, both centered at $(50, 50)$:

$$I_2(i,j) = \begin{cases} (i-50)^2 + (j-50)^2 + \epsilon, & (i-50)^2 + (j-50)^2 \leq 25^2 \\ 0.5\{(i-50)^2 + (j-50)^2\} + \epsilon, & \text{otherwise} \end{cases}, \quad (3)$$

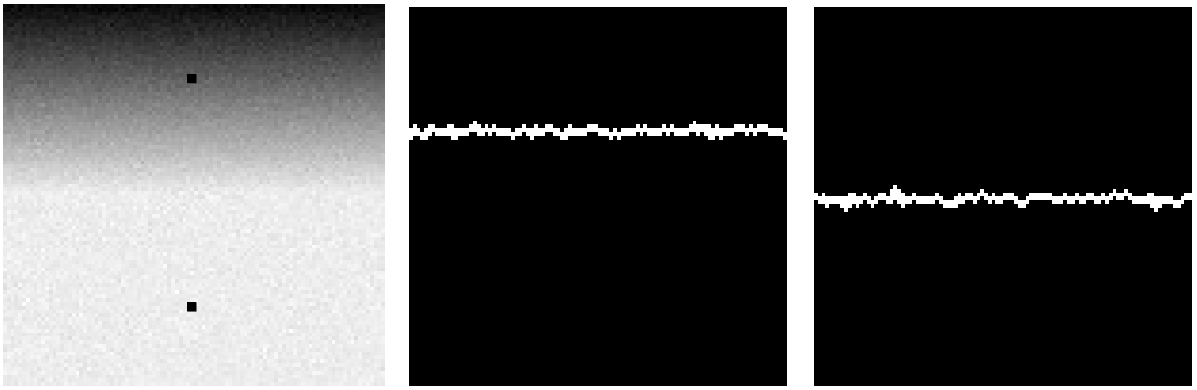

(a) (b) (c)

Figure 2: (a) Image $I_1(i,j)$ with two seeds shown as black squares. (b) Segmentation result from original SRG. (c) Segmentation result from Linear-SRG.

where the noise standard deviation is $\sigma = 2$. Figure 3 indicates that Quadratic-SRG gave superior results to the original SRG, as it nearly recovered the true boundary defined by the circle $(i-50)^2 + (j-50)^2 = 25^2$.

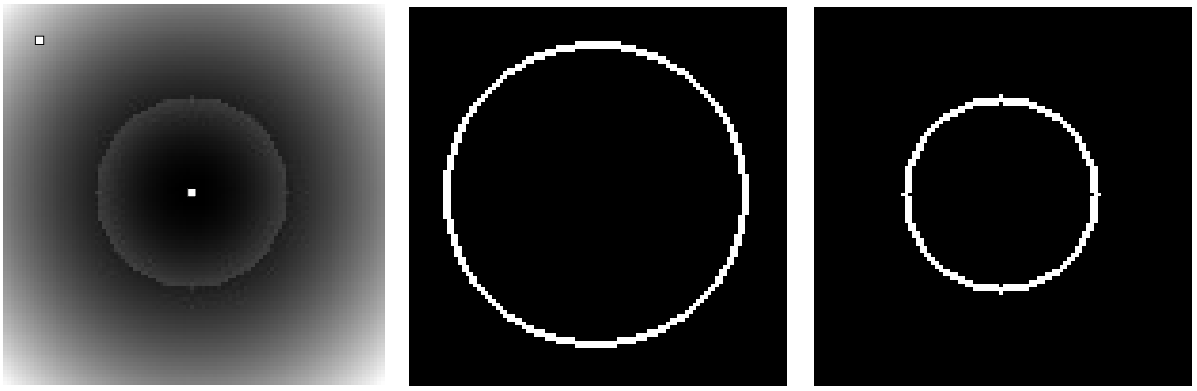

(a) (b) (c)

Figure 3: (a) Image $I_2(i,j)$ with two seeds shown as white squares. (b) Segmentation result from original SRG. (c) Segmentation result from Quadratic-SRG.

The last artificial image $I_3(i,j)$ is similar to that in [1]:

$$I_3(i,j) = \begin{cases} -10 + \epsilon, & i \in [1, 40] \\ i - 51 + \epsilon, & i \in [41, 60] \\ 10 + \epsilon, & i \in [61, 100] \end{cases},$$

where $\sigma = 10$, a relatively high level of noise. Although there are three segments in $I_3(i,j)$, it is

typically regarded as an image with two planes, with a blurred boundary at $i = 50$. Both the original SRG and Stabilized-SRG with $L = 10$ are applied and the results are given in Figure 4. It can be seen that the boundary produced by Stabilized-SRG is smoother.

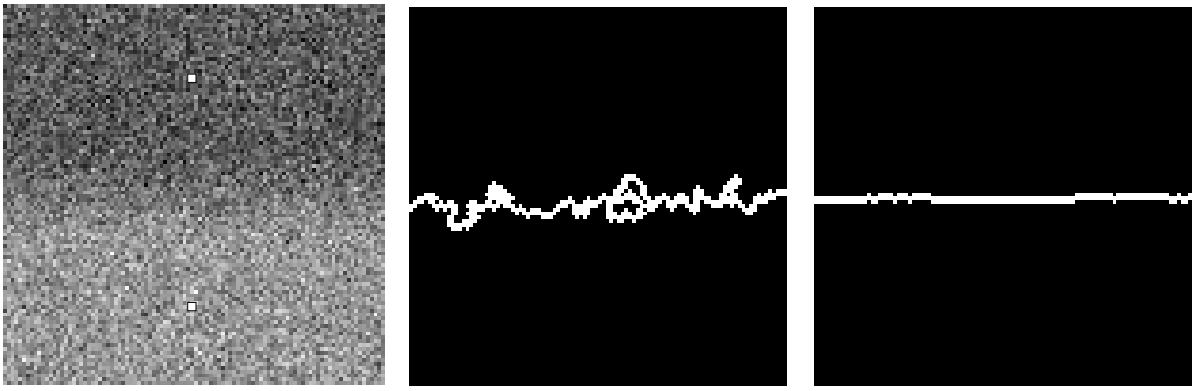

(a) (b) (c)

Figure 4: (a) Image $I_3(i, j)$ with two seeds shown as white squares. (b) Segmentation result from original SRG. (c) Segmentation result from Stabilized-SRG with $L = 10$. Notice that the "loops" in (b) are actually not loops, they are artifacts caused by how the boundary is displayed.

3.2 Real Images

In this and the next subsections real images are used to test the performances of the new SRG variants. These real images have been used by other authors as testing images; see USF Range Image Database, SAR processing tools plug-in, [13], [14], [15] and [16]. In the sequel, we will focus on the result comparisons between the original SRG and the proposed variants of SRG.

Regions in the first image are polyhedron faces and they are ideal for testing range image segmentation methods. The second image is a scenery of a beach and it would be useful to separate the sky, sand and water. Both the original SRG and Linear-SRG are applied to these images, and the results are shown in the top two rows of Figure 5. Given the fact that those regions inside these images are better modeled with linear planes, it is not surprising to see Linear-SRG outperformed the original SRG.

The third image contains a number of potatoes and quadratic modeling seems to be appropriate. The last row of Figure 5 shows the result of Quadratic-SRG, which shows a substantial improvement over the original SRG.

The fourth and fifth images under test are two synthetic aperture radar (SAR) images of a river

outlet and a rural area repectively. As with other SAR images, they are relatively noisy which would lead to rough segmented boundaries and leakages. The segmentation results from Stabilized-SRG with $L = 2$ are given in Figure 6. When comparing to results from the original SRG, Stabilized-SRG segmented the regions more accurately and with smoother boundaries.

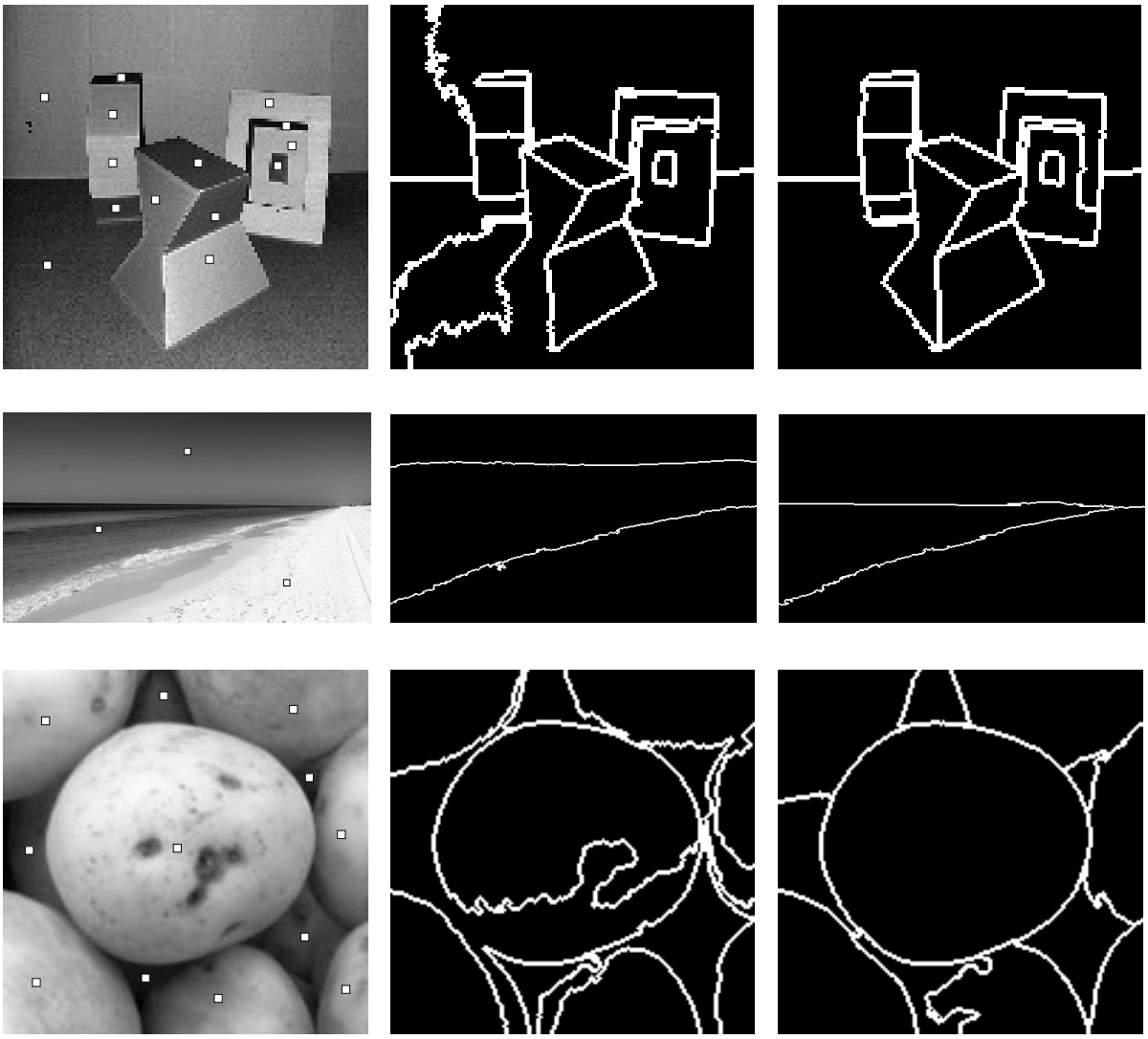

Figure 5: Left column: real images with seeds shown as white squares. Middle column: segmentation results from original SRG. Right column, top two rows: segmentation results from Linear-SRG. Right column, last row: segmentation results from Quadratic-SRG.

3.3 Mixing the Variants

This final set of numerical experiments illustrate the possibility of mixing different growing strategies together. In the first two images displayed in Figure 7, one can see that some regions can be well

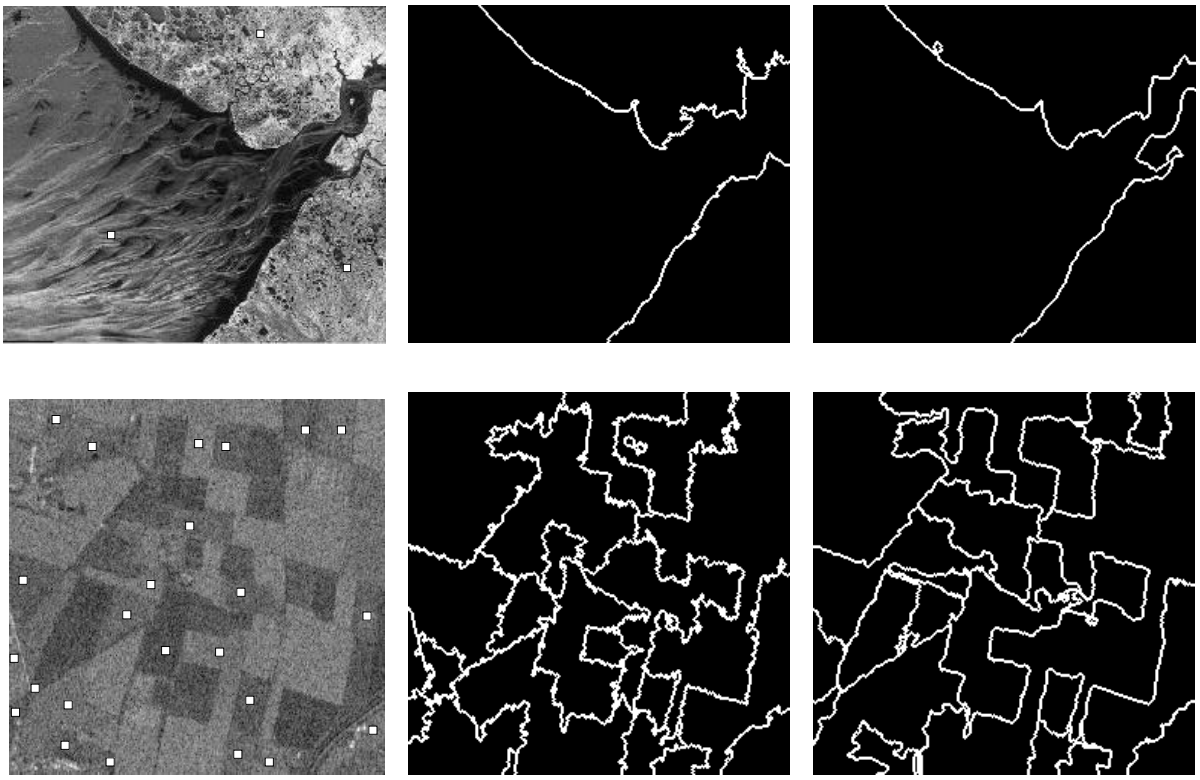

Figure 6: Left column: real images with seeds shown as white squares. Middle column: segmentation results from original SRG. Right column: segmentation results from Stabilized-SRG with $L = 2$.

approximated by horizontal planes while others by quadratic surfaces. Therefore it is natural to grow some of the regions using the original SRG, while others with Quadratic-SRG. The results are also shown in Figure 7, which suggest that the mixing strategy is superior for these two images when comparing to the original SRG.

Lastly we mix the original SRG with Stabilized-SRG. The two images under consideration are an X-ray image of a human lung and a microscope image of two biological cells; see Figure 8, which also shows the segmentation results. From these one can see that the leakage problems presented in the original SRG results are rectified by mixing with Stabilized-SRG.

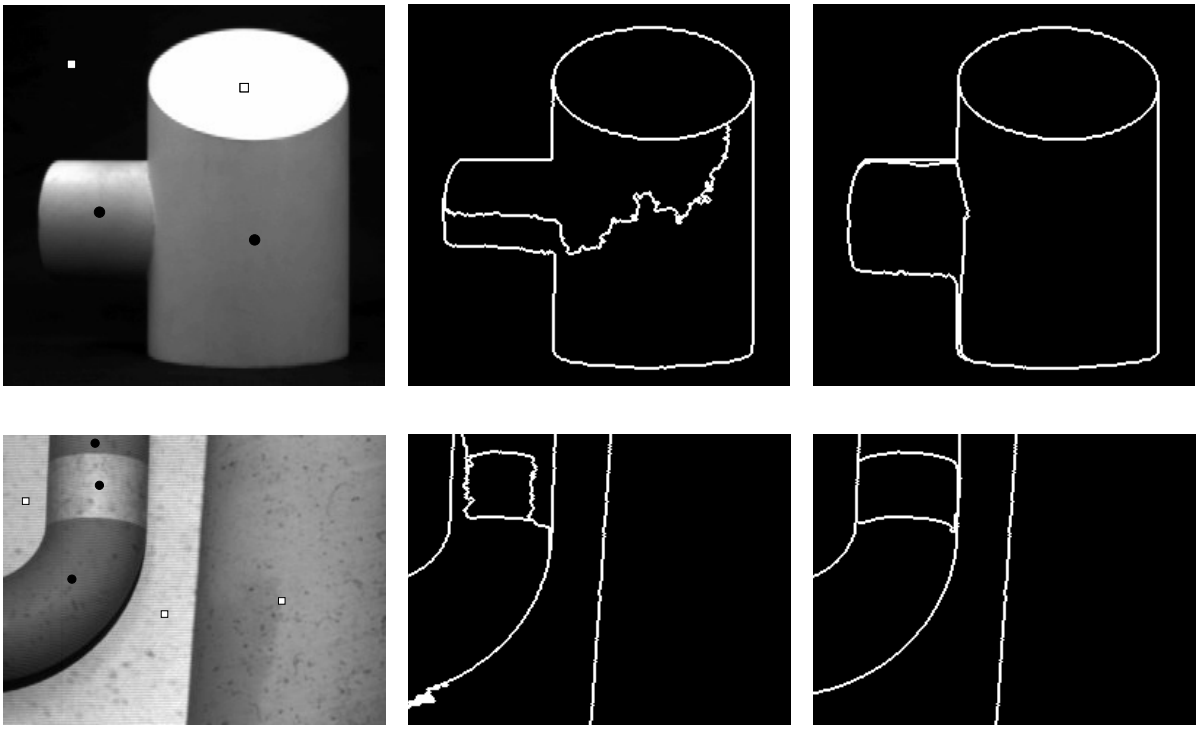

Figure 7: Left column: real images of cylinders and pipelines with seeds shown as white squares and black circles. Middle column: segmentation results when all seeds were grown using original SRG. Right column: segmentation results when the white and black seeds were grown, respectively, using original SRG and Quadratic-SRG.

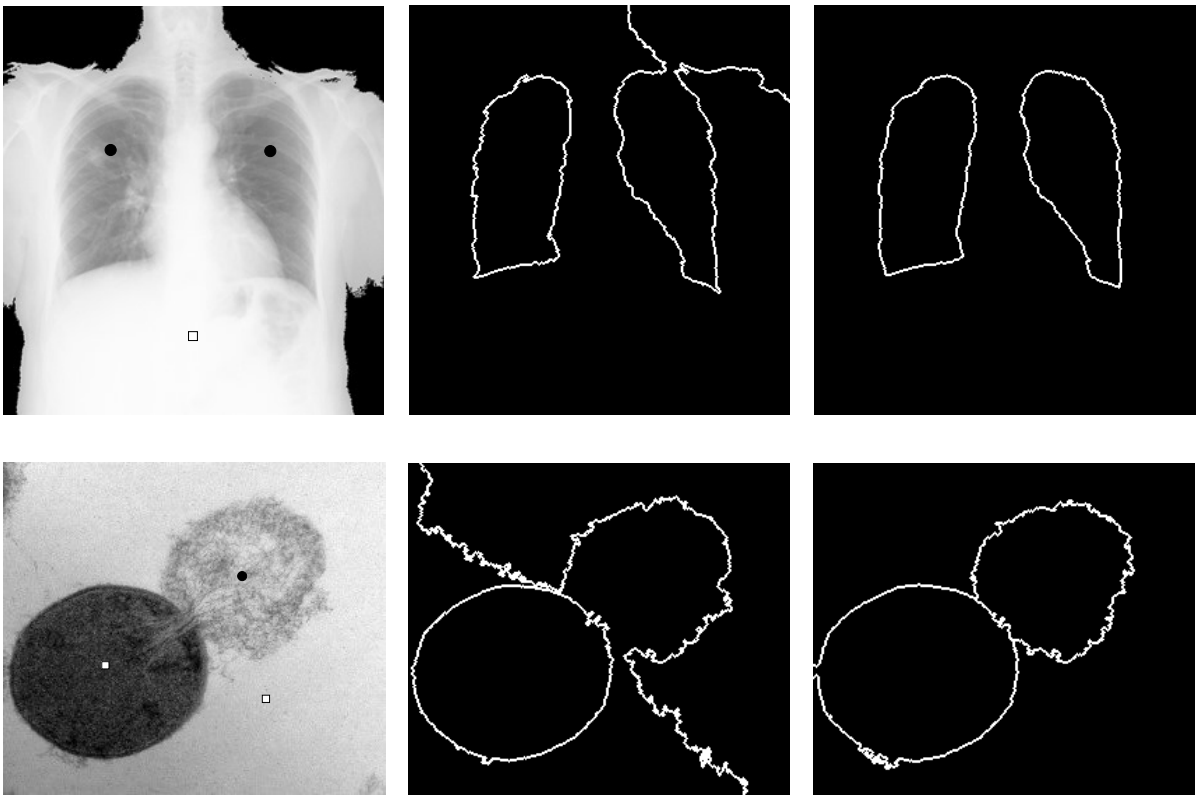

Figure 8: Left column: real images of a human lung and biological cells with seeds shown as white squares and black circles. Middle column: segmentation results when all seeds were grown using original SRG. Right column: segmentation results when the white and black seeds were grown, respectively, using original SRG and Stabilized-SRG with $L = 10$ for the first image and $L = 20$ for the second one.

3.4 Segmentation Evaluation given by F_g

Table 1 lists segmentation evaluation given by F_g for the images that have been processed by the original SRG and the variants of SRG (including Linear-SRG and Quadratic-SRG). The variants of SRG outperform the original SRG because the former always achieve smaller F_g than the latter. This conclusion is consistent with the previous supervised evaluation obtained visually.

4 Concluding Remarks

In this paper three new variants of SRG are presented: Linear-SRG, Quadratic-SRG and Stabilized-SRG. These new variants are conceptually simple and improve the performance of the original SRG under different circumstances. When the greyvalues of the regions can be well modeled by linear planes or quadratic surfaces, it is shown that Linear-SRG and Quadratic-SRG outperform the original SRG,

Table 1: Segmentation evaluation given by F_g for images processed by original SRG and variants of SRG.

Figure Index	Original SRG	Variants of SRG
Figure 2	50586	4230.6
Figure 3	6743.9	7.575
1st row of Figure 5	264900	207970
2nd row of Figure 5	196880	125050
3rd row of Figure 5	367130	312330
1st row of Figure 7	174460	86007
2nd row of Figure 7	112170	101170

while Stabilized-SRG tends to produce smoother boundaries than the original SRG in noisy images.

These variants can be further generalized. For example, they can be straightforwardly extended to multiband images (e.g., color images). For Linear-SRG and Quadratic-SRG, they can also be extended to higher order modeling, although numerical instability may pose a problem if the order is too high. For Stabilized-SRG, one could modify the shape of the neighboring set Y_L in (2); currently Y_L is a square. For example, one could use a slanted elongated shape (e.g., a rectangle or a line) to encourage stabilization in a certain direction.

The application of the proposed variants of SRG to certain cases should be careful. The first case is when the underlying assumptions of these SRG variants are violated. For example, when applying Linear-SRG or Quadratic-SRG, the regions may not be well approximated by linear planes or quadratic surfaces. In this case, more complicated geometric shapes of region surfaces should be considered. Another example for Stabilized-SRG is when the boundary between a region and the background is very blurry. In this case, even though Stabilized-SRG has the effect of leakage prevention, the leakage may still happen because of the extremely ambiguous boundary. One possible solution is to incorporate prior knowledge of the shape of the region into the learning algorithm.

Additionally, the proposed algorithms may fail when there are few pixels in a region with linear or quadratic geometric shape. Fitting this region by linear planes or quadratic surfaces would be unstable and inaccurate. In this case, we would rather apply the original SRG instead of Linear-SRG or Quadratic-SRG since taking average is more robust to the limited number of pixels.

References

[1] Adams, R., Bischof, L.: 'Seeded region growing', *IEEE Trans. Pattern Anal. Mach. Intell.*, 1994, 16, (6), pp. 641–647

[2] Justice, R.K., Stokely, E.M., Strobel, J.S., Ideker, R.E., Smith, W.M.: 'Medical image segmentation using 3d seeded region growing', *Proc. SPIE*, 1997, 3034, pp. 900–910

[3] Fan, J., Yau, D.K.Y., Elmagarmid, A.K., Member, S., Aref, W.G.: 'Automatic image segmentation by integrating color-edge extraction and seeded region growing', *IEEE Trans. Image Process.*, 2001, (10), pp. 1454–1466

[4] Grinias, I., Tziritas, G.: 'A semi-automatic seeded region growing algorithm for video object localization and tracking', *Signal Processing: Image Communication*, 2001, 16, (10), pp. 977–986

[5] Shih, F.Y., Cheng, S.: 'Automatic seeded region growing for color image segmentation', *Image and Vision Computing*, 2005, 23, (10), pp. 877–886

[6] Mehnert, A., Jackway, P.: 'An improved seeded region growing algorithm', *Pattern Recognition Letters*, 1997, 18, (10), pp. 1065–1071

[7] Beare, R.J.: 'Regularized seeded region growing', *Mathematical morphology. Proceedings of the VIth international symposium*, 2002, pp. 91–99

[8] Beare, R.: 'A locally constrained watershed transform', *IEEE Trans. Pattern Anal. Mach. Intell.*, 2006, 28, (7), pp. 1063–1074

[9] Fan, J., Zeng, G., Body, M., Hacid, M.S.: 'Seeded region growing: an extensive and comparative study', *Pattern Recognition Letters*, 2005, 26, (8), pp. 1139–1156

[10] Heimann, T., Thorn, M., Kunert, T., Meinzer, H.P.: 'New methods for leak detection and contour correction in seeded region growing segmentation', *In 20th ISPRS Congress, Istanbul 2004, International Archives of Photogrammetry and Remote Sensing*, 2004, XXXV, pp. 317–322

[11] Zhang, H., Fritts, J.E., Goldman, S.A.: 'Image segmentation evaluation: A survey of unsupervised methods', *Computer Vision and Image Understanding*, 2008, 110, (2), pp. 260–280

[12] Liu, J., Yang, Y.H.: 'Multiresolution color image segmentation', *IEEE Trans. Pattern Anal. Mach. Intell.*, 1994, 16, (7), pp. 689–700

[13] Glasbey, C.A., Mardia, K.V.: 'A penalized likelihood approach to image warping', *Journal of the Royal Statistical Society: Series B (Statistical Methodology)*, 2001, 63, (3), pp. 465–492

[14] Li, L., Zheng, Y., Kallergi, M., Clark, R.A.: 'Improved method for automatic identification of lung regions on chest radiographs', *Academic Radiology*, 2001, 8, (7), pp. 629–638

[15] Bab-Hadiashar, A., Gheissari, N.: 'Range image segmentation using surface selection criterion', *IEEE Trans. Image Process.*, 2006, 15, (7), pp. 2006–2018

[16] Aue, A., Lee, T.C.M.: 'On image segmentation using information theoretic criteria', *The Annals of Statistics*, 2011, 39, (6), pp. 2912–2935